Hindawi
Journal of Computer Networks and Communications
Volume 2018, Article ID 9575281, 14 pages
https://doi.org/10.1155/2018/9575281

Research Article

BER Performance of Stratified ACO-OFDM for Optical Wireless Communications over Multipath Channel

Zelalem Hailu Gebeyehu,[1] **Philip Kibet Langat**,[2] **and Ciira Wa Maina**[3]

[1]*Institute of Science, Technology and Innovation, Pan African University, Nairobi, Kenya*
[2]*Jomo Kenyatta University of Agriculture and Technology, Nairobi, Kenya*
[3]*Dedan Kimathi University of Technology, Nyeri, Kenya*

Correspondence should be addressed to Zelalem Hailu Gebeyehu; zelalembet@yahoo.com

Received 17 August 2017; Revised 21 January 2018; Accepted 7 February 2018; Published 1 April 2018

Academic Editor: Gianluigi Ferrari

In intensity modulation/direct detection- (IM/DD-) based optical OFDM systems, the requirement of the input signal to be real and positive unipolar imposes a reduction of system performances. Among previously proposed unipolar optical OFDM schemes for optical wireless communications (OWC), asymmetrically clipped optical OFDM (ACO-OFDM) and direct current biased optical OFDM (DCO-OFDM) are the most accepted ones. But those proposed schemes experience either spectral efficiency loss or energy efficiency loss which is a big challenge to realize high speed OWC. To improve the spectral and energy efficiencies, we previously proposed a multistratum-based stratified asymmetrically clipped optical OFDM (STACO-OFDM), and its performance was analyzed for AWGN channel. STACO-OFDM utilizes even subcarriers on the first stratum and odd subcarriers on the rest of strata to transmit multiple ACO-OFDM frames simultaneously. STACO-OFDM provides equal spectral efficiency as DCO-OFDM and better spectral efficiency compared to ACO-OFDM. In this paper, we analyze the BER performance of STACO-OFDM under the effect of multipath fading. The theoretical bit error rate (BER) bound is derived and compared with the simulation results, and good agreement is achieved. Moreover, STACO-OFDM shows better BER performance compared to ACO-OFDM and DCO-OFDM.

1. Introduction

Optical wireless communication is receiving more and more attentions from many researchers in recent years. Due to the high demand of wireless technologies, wireless data traffic in telecom network is tremendously increasing, and over-utilization of the conventional RF spectrum is becoming a big challenge. To tackle the challenge of this RF spectrum crunch, utilizing the optical spectrum for wireless communication is popularly considered to be a potential remedy. The optical spectrum intended for this application can offer wide unregulated bandwidth compared to the conventional RF spectrum. Moreover, optical wireless communication (OWC) is not easily affected by electromagnetic interference and has excellent security features [1]. The advancement of cost-effective solid state lighting technologies creates a huge motivation towards visible light communication along with illumination purpose at the same time [2]. Intensity modulation and direct detection (IM/DD) technique is the best candidate for developing low-cost OWC using the shelf transmitters and receivers.

Due to its potential of combating intersymbol interference (ISI), orthogonal frequency division multiplexing (OFDM) is confirmed as the best candidate for high speed OWC [3, 4]. The conventional complex bipolar OFDM scheme cannot be used directly for IM/DD-based OWC. Therefore, the conventional OFDM signal should be changed in to real and positive unipolar OFDM signal to make it suitable for the IM/DD system [4–9]. DCO-OFDM and ACO-OFDM are widely accepted unipolar OFDM schemes proposed for OWC on literatures [4–8]. Because of the imposed Hermitian symmetry in signal generation stage, both schemes waste 50% of the available bandwidth.

DCO-OFDM [4–6] uses additional DC bias to obtain a positive unipolar signal. But, adding a DC bias on the information signal reduces energy efficiency of the system; hence, DCO-OFDM is an energy inefficient modulation

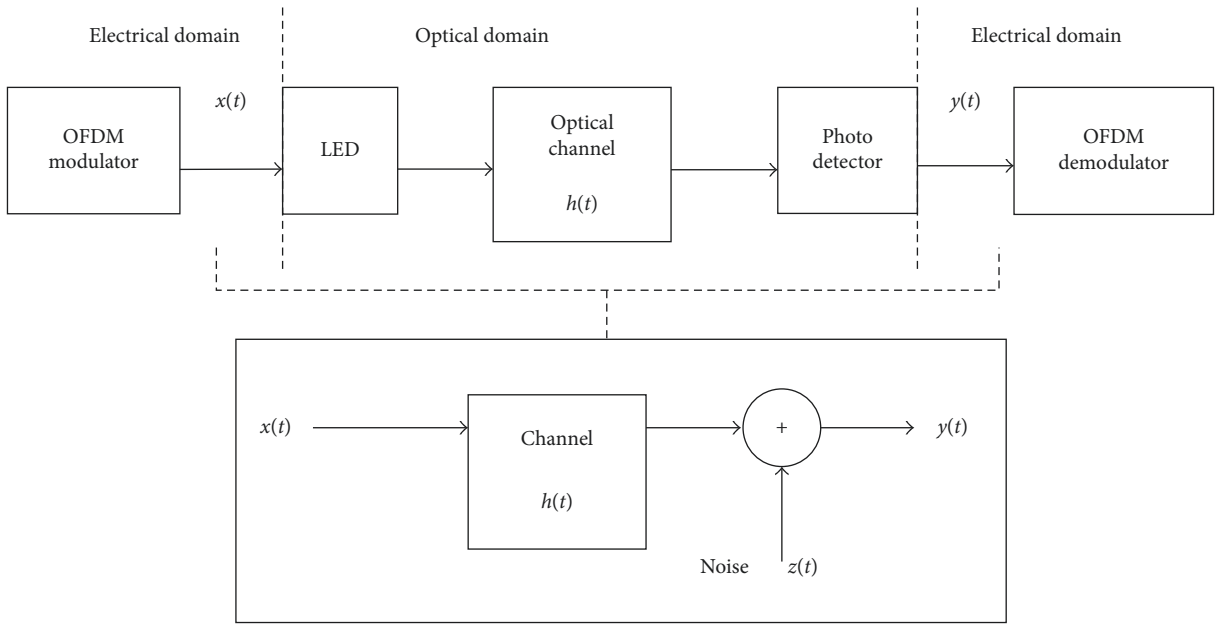

Figure 1: IM/DD system and its baseband representation.

scheme. On the contrary, ACO-OFDM [6–8] avoids a DC bias and generates a positive unipolar signal by utilizing only odd subcarriers. Since all of the even subcarriers and half of the odd subcarriers are wasted on the process, ACO-OFDM provides poor spectral efficiency compared to DCO-OFDM. In [10], we proposed STACO-OFDM to increase the data transmission rate along with the power efficiency of the OWC system. STACO-OFDM is intended to transmit multiple OFDM frames on both even and odd subcarriers simultaneously. It adopts a layered structure to use even subcarriers on the first stratum and several odd subcarriers on multiple strata. The indoor optical wireless channel has a low pass nature; therefore, utilizing both odd and even subcarriers becomes important to have more available subcarriers for data transmission in the low frequency region. STACO-OFDM has also an advantage of minimizing communication latency compared to eU-OFDM [11] which also uses a layered approach. In [10], the performance of STACO-OFDM has been analyzed and compared with the performance of ACO/DCO-OFDM in purely AWGN channel environment. The result presented on [10] reveals that STACO-OFDM can provide better BER performance compared to both ACO/DCO-OFDM on purely AWGN channel. In real world scenario, the information signal experiences multipath fading while propagating through optical wireless channel. Multipath fading is known for its challenge on the BER performance of wireless communication system during high speed communication. Due to the frequency selectivity property of the optical wireless channel, the BER performance of the overall system is degraded due to subcarriers having low channel gain. On this paper, the BER performance of STACO-OFDM is analyzed under the influence of multipath fading which is not done before. A diffused optical wireless channel configuration is considered, and ceiling bounce model is used to generate the channel impulse response (CIR).

2. System Model Descriptions

2.1. IM/DD System. Figure 1 shows IM/DD-based indoor OWC system with its equivalent baseband model. Let $x(t)$, $h(t)$, $z(t)$, and $y(t)$ represent transmitted electrical signal, the channel impulse response, the zero mean additive Gaussian noise, and the received electrical signal, respectively, and the relationship between the transmitted and the received signal can be written as follows [12]:

$$y(t) = x(t) \times h(t) + z(t). \tag{1}$$

It is noted that the IM/DD system needs $x(t)$ to be real and positive unipolar.

2.2. Diffused OWC Channel Model. In this paper, ceiling bounce model [1, 9, 13] is used to model the CIR of optical wireless channel. For diffused optical link configuration, ceiling bounce model uses a unit step function to model the CIR as follows:

$$h(t) = H(0)\frac{6a^6}{(t+a)^7}u(t), \tag{2}$$

where $a = 12(\sqrt{11/13})D_{\text{rms}}$ and D_{rms} and $H(0)$ are the channel delay spread and the DC optical gain of the channel, respectively.

2.3. DCO-OFDM. DCO-OFDM [4–6] utilizes both even and odd subcarriers for data transmission. It wastes half of the available subcarriers due to the involvement of Hermitian symmetry during the generation of real bipolar OFDM signal. For the system having N available subcarriers, the spectral efficiency Se_{DCO} of DCO-OFDM can be written as follows:

$$\text{Se}_{\text{DCO}} = \frac{\log_2 M(N-2)}{2(N+N_{\text{CP}})}, \tag{3}$$

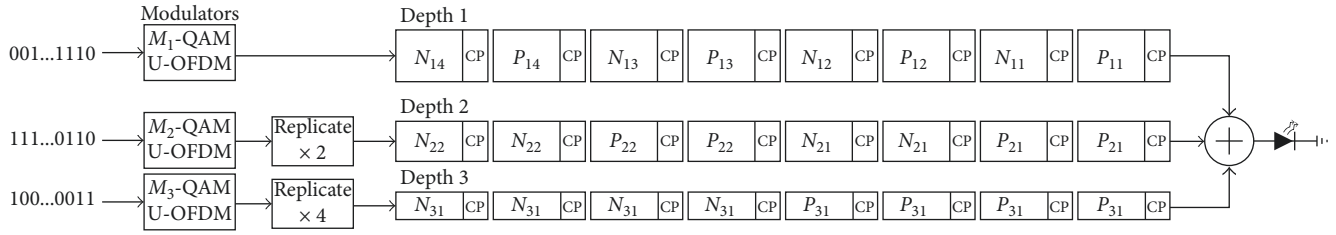

Figure 2: Frame design of eU-OFDM.

where M and N_{CP} on (3) represent the level of QAM modulation used at each subcarriers and the number of cyclic prefix, respectively. In DCO-OFDM, DC bias is added on the bipolar signal to generate a positive unipolar OFDM signal. For k amount of added DC bias, the electrical power dissipation of DCO-OFDM is increased by B_{DC} dB compared to the conventional bipolar OFDM [7]:

$$B_{DC} = 10\log_{10}\left(k^2 + 1\right). \tag{4}$$

2.4. ACO-OFDM. The conventional ACO-OFDM [6–8] utilizes only odd subcarriers for data transmission. But it is also possible to utilize only even subcarriers by leaving odd subcarriers vacant; hence, ACO-OFDM wastes either even- or odd-indexed subcarriers. The wastage of either odd or even subcarriers makes ACO-OFDM spectrally inefficient scheme compared to DCO-OFDM. For conventional M-QAM, ACO-OFDM having N subcarriers and N_{CP} cyclic prefix, the spectral efficiency is equal to

$$\mathrm{Se}_{\mathrm{ACO}}^{\mathrm{odd}} = \frac{\log_2 M(N)}{4\left(N + N_{CP}\right)}. \tag{5}$$

The above equation is only for the case of odd subcarriers that are utilized for information transmission. If only even subcarriers are utilized instead of odd subcarriers, the spectral efficiency becomes

$$\mathrm{Se}_{\mathrm{ACO}}^{\mathrm{even}} = \frac{\log_2 M(N-4)}{4\left(N + N_{CP}\right)}. \tag{6}$$

2.5. eU-OFDM. The modulation concept of eU-OFDM can be considered as the modification of unipolar OFDM (U-OFDM) [11]. In eU-OFDM scheme, multiple U-OFDM frames are superimposed together to form single time domain OFDM frame as shown in Figure 2.

Successive demodulation technique is used to recover the signal carried by all layers. The demodulation process starts from the 1st layer and then continues towards the last layer. In eU-OFDM, the signal transmission is started after enough numbers of bits are received at the transmitter for the generation of one complete eU-OFDM frame. This introduces a significant latency for real time communication which is one practicality issue of eU-OFDM. The latency introduced at the transmitter increases with the available number of layer in the system. If S is the total number of available layers in eU-OFDM, the latency of eU-OFDM at the transmitter is greater than the latency of DCO-OFDM by a factor of $2^S - 1$ for the same M-QAM modulations used on both systems. Moreover, some latency is also experienced at the receiver of eU-OFDM during successive demodulation. To demodulate the information carried by lth layer, 2^l frames should be received at the receiver. Hence, the latency is worse on higher level layers of eU-OFDM system. For enough number of available layers, the spectral efficiency, $\mathrm{Se}_{\mathrm{eU}}$, offered by eU-OFDM is equivalent to the spectral efficiency of DCO-OFDM. For the eU-OFDM system having N subcarriers and S total layers, $\mathrm{Se}_{\mathrm{eU}}$ can be given by

$$\mathrm{Se}_{\mathrm{eU}} = \sum_{l=1}^{S} \frac{\log_2\left(M_l\right)(N-2)}{2^{l+1}\left(N + N_{CP}\right)}, \tag{7}$$

where M_l and N_{CP} are the level of QAM modulation at lth layer and the number of cyclic prefix, respectively.

2.6. STACO-OFDM Signal Model. STACO-OFDM [10] utilizes both even and odd subcarriers in stratified or layered architecture. At each stratum, ACO-OFDM modulators are used, and the time domain signals from each stratum are summed up for simultaneous transmission [10]. Only even subcarriers are utilized on the first stratum while odd subcarriers are used on the rest of the strata. Due to the low pass nature of optical wireless channel, subcarriers in the low frequency region are less attenuated and affected by the multipath effect of the channel. While utilizing both even and odd subcarriers, relatively good numbers of subcarriers can be available in the low frequency region for transmission of information bits. For theoretical analysis, we consider a system having a total of S strata on which even subcarriers are used on the 1st stratum while odd subcarriers are utilized on the rest of $S-1$ strata. As given on (5) and (6), utilizing odd subcarriers on multiple strata has an advantage of maximizing the spectral efficiency since the conventional ACO-OFDM offers one additional information carrying subcarrier per stratum in comparison to even subcarrier-based ACO-OFDM. It is also noted that approximately equivalent spectral efficiency to the STACO-OFDM scheme can be achieved by utilizing only odd subcarriers on all strata. But, utilizing even subcarriers on the 1st stratum of the STACO-OFDM scheme may add further advantage and flexibility for STACO-OFDM during cellular OWC. According to [14], a significant limitation on the performance of optical attocell OWC comes from cochannel interference coming from the nearby cells using the same optical wavelength. In communication scenarios which require deployment of variable bit rate system for different

cells in optical attocell, a hybrid system which uses ACO-OFDM for low/medium data rate cells and STAC-OFDM for high data rate cells can be deployed since ACO-OFDM scheme is more economical and cost-effective for low/medium speed communications. If many superimposed symbols are loaded on odd subcarriers of STACO-OFDM in such hybrid optical attocell communication scenarios, the electrical power of those odd subcarriers will be high and will introduce a significant interference on odd subcarriers of the nearby ACO-OFDM based cells which use the same optical wavelength. Therefore, to reduce the power of each individual odd subcarriers of STACO-OFDM, significant numbers of symbols are loaded on even subcarriers at the 1st stratum to distribute the available electrical power over significantly large number of subcarriers. Hence, the interference on individual odd subcarriers of low/medium bit rate cells due to odd subcarriers of high bit rate cells will be significantly reduced. In the proposed STACO-OFDM, the length of OFDM signal is set to be $N_l = N/2^{l-1}$ at lth stratum; hence, N_l-points IFFT/FFT module is used on that specific stratum. To equalize the length of OFDM frames to N, 2^{l-1} copies of the original OFDM signal are regenerated, and two subframes with length of $N/2$ samples are constructed at the lth stratum. To transmit the complete information carried by all strata, the superposition of signal from each stratum is performed based on subframes. On this paper, when we say the 1st and 2nd subframe, we are referring to $N/2$ samples on the 1st and 2nd half of the time domain OFDM signal, respectively. After adding cyclic prefix on each subframe, the 1st subframe from each stratum is combined together and transmitted in the first transmission session. Similarly, the 2nd subframes from each stratum will be combined together and transmitted in the second transmission session. The OFDM signal generation on all strata except the 1st stratum is based on conventional ACO-OFDM while flipping of the 2nd subframe is performed at the 1st stratum. On the first stratum, even subcarriers are loaded with the M-QAM symbol while odd subcarriers are loaded with zero. The vector of M-QAM symbols, X^{s1}, loaded on the subcarriers of the 1st stratum is given as follows (Figure 3):

$$X^{s1} = \left[0, 0, X_2^{s1}, 0, X_4^{s1}, 0, \ldots, 0, X_{N_1-2}^{s1}, 0\right], \tag{8}$$

where $N_1 = N$.

The Hermitian symmetry is imposed on subcarriers to generate real OFDM signal by imposing the following relation on the loaded QAM symbols [9]:

$$X_k^{s1} = \left(X_{N-k}^{s1}\right)^*, \quad 0 < k < \frac{N}{2}. \tag{9}$$

After IFFT operation is done on loaded QAM symbols on subcarriers, the output time domain OFDM signal can be obtained. Throughout this paper, unitary IFFT/FFT operations are used to conserve equal signal power both on time and frequency domain. Therefore, the output discrete time domain OFDM signal $x^{s1}[n]$ and the frequency domain QAM symbols at the 1st stratum are related as follows [15]:

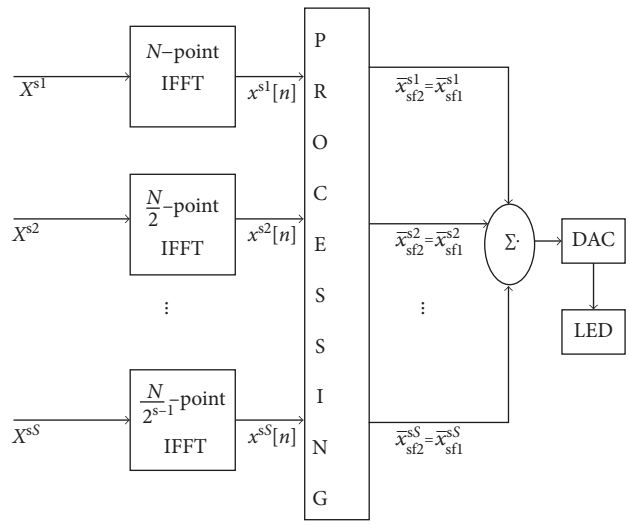

Figure 3: STACO-OFDM system model.

$$x^{s1}[n] = \frac{1}{\sqrt{N}} \sum_{k=0}^{N_1-1} X_k^{s1} \exp\left(\frac{2\pi k n}{N}\right), \quad n = 0, 1, 2, \ldots, N-1,$$

$$X_k^{s1} = \frac{1}{\sqrt{N}} \sum_{n=0}^{N-1} x^{s1}[n] \exp\left(\frac{-2\pi k n}{N}\right), \quad l = 1, 2, 3, 4, \ldots, S. \tag{10}$$

The sample values in the above equation are related with each other as follows:

$$x^{s1}[n] = x^{s1}\left[n + \frac{N}{2}\right], \quad 0 \le n \le \frac{N}{2} - 1. \tag{11}$$

To ease the interframe interference cancelation at the receiver, the entire frame of the 1st stratum is divided into two subframes with the length of $N/2$ samples each, and flipping of samples is performed on the 2nd subframe before clipping of negative samples is performed. Therefore, the two subframes $x_{sf1}^{s1}[n]$ and $x_{sf2}^{s1}[n]$ can be written as follows [10]:

$$x_{sf1}^{s1}[n] = x^{s1}[n], \quad n = 0, 1, 2, \ldots, \frac{N}{2} - 1,$$
$$x_{sf2}^{s1}[n] = -x^{s1}\left[n + \frac{N}{2}\right], \quad n = 0, 1, 2, \ldots, \frac{N}{2} - 1. \tag{12}$$

Then, after clipping the negative samples from both subframes will have clipped signals $\overline{x}_{sf1}^{s1}[n]$ and $\overline{x}_{sf2}^{s1}[n]$ as follows:

$$\overline{x}_{sf1}^{s1}[n] = \begin{cases} 0, & \text{for } x_{sf1}^{s1}[n] \le 0,\ n = 0, 1, 2, \ldots, \frac{N}{2} - 1 \\ x_{sf1}^{s1}[n], & \text{for } x_{sf1}^{s1} > 0,\ n = 0, 1, 2, \ldots, \frac{N}{2} - 1, \end{cases}$$

$$\overline{x}_{sf2}^{s1}[n] = \begin{cases} 0, & \text{for } x_{sf2}^{s1}[n] \le 0,\ n = 0, 1, 2, \ldots, \frac{N}{2} - 1 \\ x_{sf2}^{s1}[n], & \text{for } x_{sf2}^{s1} > 0,\ n = 0, 1, 2, \ldots, \frac{N}{2} - 1. \end{cases} \tag{13}$$

Now after adding cyclic prefix on each subframe, the two subframes of 1st stratum are ready to be combined with subframes from higher strata. In the rest of strata, only odd subcarriers are loaded with M-QAM symbols while even subcarriers are loaded with zero QAM symbols.

For example, let us consider X^{sl} is the frequency domain QAM symbols loaded on subcarriers at lth stratum where $l \neq 1$ (the superscripts sl stand for stratum – l or lth stratum). Then, X^{sl} which is the vector of QAM symbols loaded on the lth stratum is given as follows:

$$X^{sl} = \left[0, X_1^{s2}, 0, X_3^{s2}, 0, \ldots, 0, X_{N_l-1}^{s2}\right], \tag{14}$$

where $N_l = N/2^{l-1}$, $l = 2, 3, 4, \ldots, S$.

From the above equation, it is noted that the even subcarriers are left empty while the odd subcarriers are loaded with QAM symbols. The Hermitian symmetry is introduced by imposing the following relations on the loaded QAM symbols for enabling the generation of real bipolar signal [9]:

$$X_k^{sl} = \left(X_{N_l-k}^{sl}\right)^*, \quad 0 < k < \frac{N_l}{2}. \tag{15}$$

After taking IFFT, the time domain OFDM signal $x^{sl}[n]$ is obtained at the lth stratum as follows:

$$x^{sl}[n] = \frac{1}{\sqrt{N_l}} \sum_{k=0}^{N_l-1} X_k^{sl} \exp\left(\frac{2\pi k n}{N_l}\right), \quad l = 2, 3, 4, \ldots, S. \tag{16}$$

To equalize the length of time domain signal at each stratum to N, $x^{sl}[n]$ is replicated to generate 2^{l-1} exact copies at the lth stratum. To conserve equal frame energy before and after the replication process, the original frame at the lth stratum should be scaled by a factor of $1/\sqrt{2^{l-1}}$. The 2^{l-2} copies are then merged together to form $x_{sf1}^{sl}[n]$ and $x_{sf2}^{sl}[n]$ which are the 1st and 2nd subframes of the lth stratum, respectively. Clipping of negative samples and adding of cyclic prefixes are then done on the 1st and the 2nd subframes of all strata. Clipping of negative samples can be performed using the following operation:

$$\overline{x}_{sf1}^{sl}[n] = \begin{cases} 0, & \text{for } x_{sf1}^{sl}[n] \leq 0, \quad n = 0, 1, 2, \ldots, \dfrac{N}{2} - 1, \quad l = 2, 3, 4, \ldots, S \\ x_{sf1}^{sl}[n], & \text{for } x_{sf1}^{sl} > 0, \quad n = 0, 1, 2, \ldots, \dfrac{N}{2} - 1, \quad l = 2, 3, 4, \ldots, S, \end{cases}$$

$$\overline{x}_{sf2}^{sl}[n] = \begin{cases} 0, & \text{for } x_{sf2}^{sl}[n] \leq 0, \quad n = 0, 1, 2, \ldots, \dfrac{N}{2} - 1, \quad l = 2, 3, 4, \ldots, S \\ x_{sf2}^{sl}[n], & \text{for } x_{sf2}^{sl} > 0, \quad n = 0, 1, 2, \ldots, \dfrac{N}{2} - 1, \quad l = 2, 3, 4, \ldots, S, \end{cases} \tag{17}$$

where $\overline{x}_{sf1}^{sl}[n]$ and $\overline{x}_{sf2}^{sl}[n]$ are the 1st and the 2nd subframes, respectively, at the lth stratum after clipping of negative samples. The entire frame of STACO-OFDM is transmitted in two successive transmission sessions. The 1st subframes from each stratum are combined together to form $x_{t1}[n]$ to be transmitted in the 1st transmission session, and $x_{t1}[n]$ can be written as

$$x_{t1}[n] = \sum_{l=1}^{S} \overline{x}_{sf1}^{sl}[n]. \tag{18}$$

Similarly, for the second transmission session, $x_{t2}[n]$ is formed by summing the 2nd subframes of all strata as

$$x_{t2}[n] = \sum_{l=1}^{S} \overline{x}_{sf2}^{sl}[n]. \tag{19}$$

At the receiver of STAC-OFDM, there are two received signals, $x_{r1}[n]$ and $x_{r2}[n]$, from two consecutive transmission sessions as follows [12]:

$$\begin{aligned} x_{r1}[n] &= x_{t1}[n] \times h[n] + z_1[n], \\ x_{r2}[n] &= x_{t2}[n] \times h[n] + z_2[n], \end{aligned} \tag{20}$$

where $h[n]$ and $z_1[n]$ and $z_2[n]$ are the channel impulse response and the AWGN signal added on the 1st and the 2nd subframes, respectively. The demodulation process is performed by adopting successive demodulation technique stratum by stratum [11, 16]. The 1st stratum information recovery is begun by subtracting $x_{r2}[n]$ from $x_{r1}[n]$. After doing the subtraction, the output signal $x_r^{s1}[n]$ becomes

$$\begin{aligned} x_r^{s1}[n] &= x_{r1}[n] - x_{r2}[n] \\ &= \left(x_{t1}[n] - x_{t2}[n]\right) \times h[n] + \left(z_1[n] - z_2[n]\right) \\ &= \left(x_{sf1}^{s1}[n] - x_{sf2}^{s1}[n]\right) \times h[n] + z[n] \\ &= x^{\text{diff}}[n] \times h[n] + z[n]. \end{aligned} \tag{21}$$

On the above equation, $z[n]$ is the AWGN noise with single-sided noise spectral density N_0 which is added in one complete OFDM frame, and $x^{\text{diff}}[n]$ is the bipolar signal which is exactly equal to the 1st half of $x^{s1}[n]$. In addition, the length of $x^{\text{diff}}[n]$ is equal to $(N/2) + N_{\text{CP}}$, and the length of $h[n]$ is equal to L, where $N_{\text{CP}} \geq L$, $h[n]$ is equal to zero for $n > L$. Therefore, the channel impulse response $h(l)$ can be written in vector form as

$$h(l) = \underbrace{[h[0]\, h[1]\, h[2] \cdots h[L-1]\, 0\, 0\, 0 \cdots 0]}_{(N/2)\text{ samples}}. \quad (22)$$

But we can write (21) by using summation as [17]

$$x_{\mathrm{r}}^{\mathrm{s1}}[n] = \sum_{l=0}^{L-1} h[l]\, x^{\mathrm{diff}}[n-l] + z[n], \quad n = 0, 1, 2, \ldots, \frac{N}{2} + N_{\mathrm{CP}}. \quad (23)$$

The matrix representation for the above (23) becomes [17, 18]

$$\left[x_{\mathrm{r}}^{\mathrm{s1}}\right] = [h]\left[x^{\mathrm{diff}}\right] + [z], \quad (24)$$

where $[x_{\mathrm{r}}^{\mathrm{s1}}]$, $[x^{\mathrm{diff}}]$, and $[z]$ are $((N/2) + N_{\mathrm{CP}}) \times 1$ matrices while $[h]$ is $((N/2) + N_{\mathrm{CP}}) \times ((N/2) + N_{\mathrm{CP}})$ matrix. To recover the information carried by the 1st stratum, $[x_{\mathrm{r}}^{\mathrm{s1}}]$ is given to N-point FFT module after removing the first N_{CP} long samples from $[x_{\mathrm{r}}^{\mathrm{s1}}]$. But it is also noted that the N-point FFT module will pad $N/2$ zeros by default at the end of $[x_{\mathrm{r}}^{\mathrm{s1}}]$. After the default zero padding, $[x_{\mathrm{r}}^{\mathrm{s1}}]$, $[x^{\mathrm{diff}}]$, and $[z]$ become $N \times 1$ matrices and their last $N/2$ rows are zero valued. Similarly, $[h]$ becomes an $N \times N$ matrix. But $[x^{\mathrm{diff}}]$ is exactly similar to $[x^{\mathrm{s1}}] = x^{\mathrm{s1}}[n]^T$ in which its last $N/2$ samples are clipped to zero. According to [8], the clipped signal can be given by

$$\left[x^{\mathrm{diff}}\right] = R\left[x^{\mathrm{s1}}\right] + [d], \quad (25)$$

where R is a constant which is equal to 0.5, and $[d]$ is the clipping noise which is $N \times 1$ matrix, but we can write $[x^{\mathrm{s1}}]$ in terms of IFFT matrix F^{-1} and the frequency domain QAM symbol vector $[X^{\mathrm{s1}}]$ as follows [18]:

$$\left[x^{\mathrm{diff}}\right] = RF^{-1}\left[X^{\mathrm{s1}}\right] + [d]. \quad (26)$$

Substituting (26) into (24), the result becomes

$$\left[x_{\mathrm{r}}^{\mathrm{s1}}\right] = RF^{-1}[h]\left[X^{\mathrm{s1}}\right] + [d] + [z]. \quad (27)$$

Taking FFT operation on the above signal by using FFT matrix F [18],

$$\begin{aligned} F\left[x_{\mathrm{r}}^{\mathrm{s1}}\right] &= RF^{-1}[h]F\left[X^{\mathrm{s1}}\right] + F[d] + F[z] \\ &= R[C]\left[X^{\mathrm{s1}}\right] + F[d] + F[z], \end{aligned} \quad (28)$$

where $[C] = F^{-1}[h]F$ is a diagonal matrix whose diagonal is equal to the Fourier transform of the channel impulse response $h[n]$ as

$$H_k = F\{h[n]\}, \quad k, n = 0, 1, 2, \ldots, N-1. \quad (29)$$

The received frequency domain signal at each subcarriers on the 1st stratum becomes

$$Y_k^{\mathrm{s1}} = RH_k X_k^{\mathrm{s1}} + D_k + Z_k, \quad k = 0, 1, 2, \ldots, N-1. \quad (30)$$

Introducing zero forcing equalization for reducing the channel effect [12, 19],

$$\frac{Y_k^{\mathrm{s1}}}{RH_k} = X_k^{\mathrm{s1}} + \frac{D_k}{RH_k} + \frac{Z_k}{RH_k}, \quad k = 0, 1, \ldots, N-1. \quad (31)$$

On the above equation, it is also noted that the clipping noise only affects the odd subcarriers [8, 10]. Since the even subcarriers are not affected by the clipping noise, we can write the received symbols on the even subcarriers at the 1st stratum as

$$\frac{Y_k^{\mathrm{s1}}}{RH_k} = X_k^{\mathrm{s1}} + \frac{Z_k}{RH_k}, \quad k = 2, 4, 6, \ldots, N-2. \quad (32)$$

The information bits carried by the 1st stratum can be recovered by demodulating the above symbols received on even subcarriers. To recover the information carried by the 2nd stratum, the recovered bits at the 1st stratum should be remodulated again and processed in the same way as it was done at the transmitter. The remodulated time domain subframes are then affected by the CIR of the channel and subtracted from $x_{\mathrm{r1}}[n]$ and $x_{\mathrm{r2}}[n]$ to remove the contribution of the 1st stratum. By following similar mathematical analysis as it was done for the 1st stratum, the equalized QAM symbols received on odd subcarriers of the 2nd stratum will be in the following form:

$$\frac{Y_k^{\mathrm{s2}}}{RH_k} = X_k^{\mathrm{s2}} + \frac{Z_k}{RH_k}, \quad k = 1, 3, 5, \ldots, \frac{N}{2} - 1. \quad (33)$$

Then, by demodulating the above resulted symbols after subtraction by conventional ACO-OFDM demodulator, it is possible to recover the information signal from odd subcarriers. Similarly, by remodulating the bits recovered at the 2nd stratum and subtracting it from the received signal, the equalized QAM symbols received on the 3rd stratum can be written as

$$\frac{Y_k^{\mathrm{s3}}}{RH_k} = X_k^{\mathrm{s3}} + \frac{Z_k}{RH_k}, \quad k = 1, 3, \ldots, \frac{N}{4} - 1. \quad (34)$$

Then, the bits stream carried by the 3rd stratum can be recovered by demodulating the above symbols using the QAM demodulator. The bits carried by the other strata can also be recovered by using the same strategy stratum by stratum.

Due to its efficient signal generation and demodulation strategies, STACO-OFDM has lower system latency compared to eU-OFDM. For same M-QAM modulation used on all of the available S strata of both eU-OFDM and STACO-OFDM schemes, the latency introduced at the transmitter of STACO-OFDM scheme is approximately less than the latency experienced at the transmitter of eU-OFDM by a factor of $2^S - 1$. For example, if we consider $S = 3$ for both schemes, $7(\log_2 M)(N/2 - 1)$ bits should be received at the transmitter of eU-OFDM before transmission while $(\log_2 M)(7N/16 - 1)$ bits are enough for the case of STACO-OFDM. Furthermore, the latency introduced at the receiver of STACO-OFDM is also lower compared to eU-OFDM since the frame length of STACO-OFDM scheme is less than the frame length of eU-OFDM by a factor of 2^S as shown in Figures 2 and 4. Therefore, STACO-OFDM scheme has better advantage over eU-OFDM for latency sensitive real-time communications.

Furthermore, implementing one tap frequency domain channel equalization is easier in STACO-OFDM than in eU-OFDM. To perform frequency domain channel equalization on the lth layer of eU-OFDM, the CIR of the channel

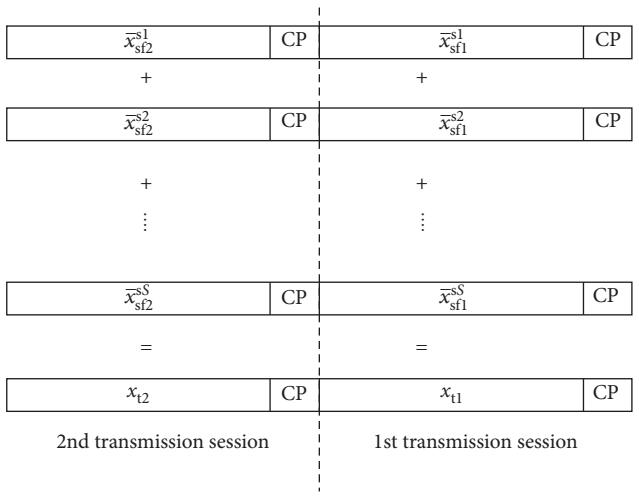

Figure 4: STACO-OFDM frame design.

should be constant throughout 8 frames duration. On contrary, the channel effect can be equalized successfully in STACO-OFDM as long as the channel is invariant over one frame duration. Therefore, STACO-OFDM can be used on applications involving fast channel dynamics scenario.

3. Spectral Efficiency of STACO-OFDM

The spectral efficiency of STACO-OFDM can be calculated as the summation of the spectral efficiencies delivered by all available strata. The spectral efficiency Se_l offered by the lth stratum is given by [10]

$$\mathrm{Se}_l = \begin{cases} \dfrac{(\log_2 M_l)(N-4)}{4(N+N_{\mathrm{CP}})}, & l = 1 \\ \dfrac{(\log_2 M_1)(N)}{2^{l+1}(N+N_{\mathrm{CP}})}, & l \neq 1. \end{cases} \tag{35}$$

Then, the total spectral efficiency Se of STACO-OFDM can be calculated as follows:

$$\mathrm{Se} = \sum_{l=1}^{S} \mathrm{Se}_l. \tag{36}$$

STACO-OFDM has equivalent spectral efficiency with eU-OFDM and DCO-OFDM schemes, and it can offer better spectral efficiency compared to ACO OFDM.

4. Theoretical BER Bound of STACO-OFDM

4.1. BER Interms of Electrical SNR. It is known that the real bipolar time domain OFDM signal at each stratum has a Gaussian distribution for enough number of available subcarriers [20]. The average electrical power of the OFDM signal at the lth stratum is equal to σ_l^2 which is the variance of the signal samples distribution. Therefore, the average transmitted electrical power P_l of the bipolar signal at the lth stratum is given by

$$P_l = \sigma_l^2 = \int_{-\infty}^{\infty} m^2 f_l(m)\, dm, \tag{37}$$

where $f_l(m)$ is the probability density function (PDF) of the signal at the lth stratum and given by [20]

$$f_l(m) = \frac{1}{\sqrt{2\pi}\sigma_l} e^{-m^2/2\sigma_l^2}, \quad l = 1, 2, 3, \ldots, S. \tag{38}$$

Let $x_l[n]$ is the complete frame signal at lth stratum after clipping and scaling of the signal for conserving the symbol energy, so $x_l[n]$ can be written by merging the two subframes as

$$x_l[n] = \left[\bar{x}_{\mathrm{sf1}}^{sl}\ \bar{x}_{\mathrm{sf2}}^{sl}\right], \quad l = 1, 2, 3, \ldots, S. \tag{39}$$

The clipping of negative samples reduces the average electrical power by a factor of 1/2 compared to the bipolar signal. The average electrical power $P_l^{'}$ of the time domain signal $x_l[n]$ at the lth stratum becomes:

$$P_l^{'} = E\left[x_l^2[n]\right] = \frac{1}{2}\left(\frac{P_l}{2^{l-1}}\right) = \frac{\sigma_l^2}{2^l}, \quad l = 1, 2, \ldots, S. \tag{40}$$

In (40), the factors 1/2 and $1/2^{l-1}$ come from the clipping of negative samples and the scaling of signal, respectively. Considering $x_T[n]$ is the aggregate OFDM signal after combining the OFDM signals from all strata as

$$x_T[n] = \sum_{l=1}^{S} x_l[n]. \tag{41}$$

The average electrical power $P_{\mathrm{el}}^{\mathrm{avg}}$ of the combined OFDM signal $x_T[n]$ becomes [11, 20, 21]

$$\begin{aligned} P_{\mathrm{el}}^{\mathrm{avg}} &= E\left[x_T^2[n]\right] = E\left[\left(\sum_{l=1}^{S} x_l[n]\right)^2\right] \\ &= \sum_{l=1}^{S} E\left[x_l^2[n]\right] + \sum_{l_1=1}^{S} \sum_{\substack{l_2=1 \\ l_1 \neq l_2}}^{S} E\left[x_{l_1}[n]\right] E\left[x_{l_2}[n]\right] \\ &= \sum_{l=1}^{S} \frac{\sigma_l^2}{2^l} + \sum_{l_1=1}^{S} \sum_{\substack{l_2=1 \\ l_1 \neq l_2}}^{S} \left(\frac{\sigma_{l_1}}{\sqrt{2^{l_1}\pi}}\right)\left(\frac{\sigma_{l_2}}{\sqrt{2^{l_2}\pi}}\right) \\ &= \sum_{l=1}^{S} \frac{\sigma_l^2}{2^l} + \frac{1}{\pi} \sum_{l_1=1}^{S} \sum_{\substack{l_2=1 \\ l_1 \neq l_2}}^{S} \frac{\sigma_{l_1}\sigma_{l_2}}{\sqrt{2^{l_1+l_2}}}. \end{aligned} \tag{42}$$

The average achieved SNR per bit at the kth subcarrier of the entire combined system is given by [11, 16]

$$\gamma_k = \frac{\left|H_k\right|^2 P_{\mathrm{el}}^{\mathrm{avg}}}{BN_0(Se)}. \tag{43}$$

But the SNR per bit at the kth subcarrier has different values at different strata; the SNR per bit at the kth subcarrier of the lth stratum can be given by

$$\gamma_{l,k} = \frac{|H_k|^2 P_l'}{BN_0(\mathrm{Se}_l)}, \tag{44}$$

where P_l' is the electrical power of the clipped signal at the lth stratum which is equal to $\sigma_l^2/2$. The theoretical BER at the kth subcarrier of the lth stratum can be given by the BER formula of M-QAM modulation as follows [22]:

$$\mathrm{BER}_{l,k} = \frac{4}{\log_2 M_l}\left(1 - \frac{1}{\sqrt{M_l}}\right)\sum_{i=1}^{\sqrt{M_l}/2} Q\left((2i-1)\sqrt{\frac{3\log_2 M_l \gamma_{l,k}}{M_l - 1}}\right). \tag{45}$$

From the above equation, the overall BER at the lth stratum can be calculated as

$$\mathrm{BER}_l = \frac{1}{N_l^{\mathrm{info}}}\sum_{k=1}^{(N_l/2)-1} \mathrm{BER}_{l,k}, \quad l = 1, 2, 3, \ldots, S, \tag{46}$$

where N_l^{info} is the number of information-carrying subcarriers at the lth stratum. For the 1st stratum (i.e., $l = 1$), k is even as $k = 2, 4, 6, \ldots, (N/2) - 2$ since only even subcarriers are carrying information. For the rest of the strata, k is odd as $k = 1, 3, 5, \ldots, (N_l/2) - 1$.

The theoretical BER bound of STACO-OFDM on multipath channel can be derived from the theoretical BER bound achieved at the available strata. Let S and N_l^{bits} stand for the total number of used strata and the total number of bits transmitted at the lth stratum in one complete OFDM frame transmission, respectively, the BER of the overall STACO-OFDM system is then given by [10]

$$\begin{aligned}\mathrm{BER}_{\mathrm{tot}} &= \frac{\text{total number of erroneous bits per STACO-OFDM frame}}{\text{total number of transmitted bits per STACO-OFDM frame}} \\ &= \frac{\sum_{l=1}^{S}(\mathrm{BER}_l N_l^{\mathrm{bits}})}{\sum_{s=1}^{S} N_l^{\mathrm{bits}}}.\end{aligned} \tag{47}$$

4.2. BER Interms of Optical Power of Transmitted Signal. Percival's theorem can be applied at each stratum since unitary IFFT/FFT is used on each stratum [15]. Therefore, at any lth stratum, the electrical power is equal in time and frequency domain as

$$E\left[\sum_{k=0}^{N-1}\left|X_k^{sl}\right|^2\right] = E\left[\sum_{n=0}^{N-1}\left|x^{sl}[n]\right|^2\right] = \sum_{n=0}^{N-1} E\left[\left|x^{sl}[n]\right|^2\right]. \tag{48}$$

According to the above equation, the average electrical power of the bipolar signal at the lth stratum can be calculated as

$$\begin{aligned}P_l &= \frac{1}{N_l}\sum_{n=0}^{N_l-1} E\left[\left|x^{sl}[n]\right|^2\right] \\ &= \frac{2^{l-1}}{N}\sum_{n=0}^{(N/2^{l-1})-1} E\left[\left|x^{sl}[n]\right|^2\right] \\ &= \sigma_l^2,\end{aligned} \tag{49}$$

where $l = 1, 2, 3, \ldots, S$.

But from (48) and (49), we have

$$\begin{aligned}\frac{2^{l-1}}{N}\sum_{n=0}^{(N/2^{l-1})-1} E\left[\left|x^{sl}[n]\right|^2\right] &= \frac{2^{l-1}}{N} E\left[\sum_{k=0}^{(N/2^{l-1})-1}\left|X_k^{sl}\right|^2\right] \\ &= \sigma_l^2,\end{aligned} \tag{50}$$

where $l = 1, 2, 3, \ldots, S$.

Then, after clipping the negative samples of the signal, the average electrical power P_l' of the unipolar signal at the lth stratum will equal to the average symbol power of the clipped symbol $\overline{X}_k^l$ as

$$\begin{aligned}P_l' &= \frac{2^{l-1}}{N} E\left[\sum_{k=0}^{(N/2^{l-1})-1}\left|\overline{X}_k^{sl}\right|^2\right] \\ &= \frac{\sigma_l^2}{2},\end{aligned} \tag{51}$$

where $l = 1, 2, \ldots, S$.

Similarly, the average optical power of the transmitted signal on the lth stratum can be calculated as mean of truncated random variables [11, 21]:

$$P_l^{\mathrm{o}} = E[x_l[n]] = \frac{\sigma_l}{\sqrt{\pi 2^l}}, \quad l = 1, 2, 3, \ldots, S. \tag{52}$$

But using (51) and (52), we can write P_l' as

$$P_l' = \pi\left(2^{l-1}\right)\left(P_l^{\mathrm{o}}\right)^2, \quad l = 1, 2, 3, \ldots, S. \tag{53}$$

Then, it is possible to write P_l' as

$$\begin{aligned}P_l' &= \frac{2^{l-1}}{N} E\left[\sum_{k=0}^{(N/2^{l-1})-1}\left|\overline{X}_k^{sl}\right|^2\right] \\ &= \pi\left(2^{l-1}\right)\left(P_l^{\mathrm{o}}\right)^2,\end{aligned} \tag{54}$$

where $l = 1, 2, 3, \ldots, S$.

If we assume all the clipped version of QAM symbols on subcarriers at the lth stratum have equal average electrical power, we will have

$$E\left[\left|\overline{X}_k^{sl}\right|^2\right] = \pi\left(2^{l-1}\right)\left(P_l^{\mathrm{o}}\right)^2. \quad (55)$$

Then, at the receiver, the transmitted clipped QAM symbol at the kth subcarrier of lth stratum is further attenuated by the channel gain $|H_k|$; hence, the received QAM symbol Y_k^{sl} at the kth subcarrier of the lth stratum will have average electrical power of

$$E\left[\left|Y_k^{sl}\right|^2\right] = \left|H_k\right|^2 E\left[\left|\overline{X}_k^{sl}\right|^2\right] = \pi\left(2^{l-1}\right)\left(P_l^{\mathrm{o}}\right)^2\left|H_k\right|^2. \quad (56)$$

To calculate the effective SNR of the QAM symbol received at the kth subcarrier, the AWGN noise power at kth the subcarrier should be known. Let N_0 be the single-sided noise spectral density; the noise variance σ_z^2 at each subcarriers is given by [15]

$$\sigma_z^2 = E\left[\left|Z_k\right|^2\right] = \left(\frac{N_0 B_{\mathrm{sc}}}{2}\right)\left(\frac{N}{2^{l-1}}\right), \quad l = 1, 2, \ldots, S, \quad (57)$$

where B_{sc} is the bandwidth of subcarrier, and $N/2^{l-1}$ term comes from the definition of the unitary IFFT/FFT algorithm. The SNR of the symbol received at the kth subcarrier is then given by [7, 15]

$$\mathrm{SNR}_k = \frac{E\left[\left|Y_k^{sl}\right|^2\right]}{\sigma_z^2} = \frac{2^{2l-1}\pi\left(P_l^{\mathrm{o}}\right)^2\left|H_k\right|^2}{N_0 B_{\mathrm{sc}} N}, \quad l = 1, 2, \ldots, S. \quad (58)$$

But for more simplicity, writing SNR_k in terms of the total average optical power of the combined signal is vital. The average optical power $P_{\mathrm{o}}^{\mathrm{avg}}$ of the combined signal $x_T(t)$ can be given by [11, 21]

$$P_{\mathrm{o}}^{\mathrm{avg}} = E\left[x_T[n]\right] = E\left[\sum_{l=1}^{S} x_l[n]\right] = \sum_{l=1}^{S} \frac{\sigma_l}{\sqrt{\pi 2^l}}. \quad (59)$$

The optical power penalty of the combined system with respect to the optical power at the lth stratum can be written as follows:

$$\alpha_l^{\mathrm{o}} = \frac{\left(P_{\mathrm{o}}^{\mathrm{avg}}\right)^2}{\left(P_l^{\mathrm{o}}\right)^2}, \quad l = 1, 2, \ldots, S. \quad (60)$$

Therefore, SNR_k can be written in terms of the overall transmitted optical power of STACO-OFDM system as follows:

$$\mathrm{SNR}_k = \frac{2^{2l-1}\pi\left(P_{\mathrm{o}}^{\mathrm{avg}}\right)^2\left|H_k\right|^2}{N_0 B_{\mathrm{sc}} N \alpha_l^{\mathrm{o}}}, \quad l = 1, 2, \ldots, S. \quad (61)$$

The SNR per bit $\gamma_{l,k}$ can also be calculated as

$$\gamma_{l,k} = \frac{\mathrm{SNR}_{l,k}}{\log_2 M_l} = \frac{2^{2l-1}\pi\left(P_{\mathrm{o}}^{\mathrm{avg}}\right)^2\left|H_k\right|^2}{N_0 B_{\mathrm{sc}} N \alpha_l^{\mathrm{o}}\left(\log_2 M_l\right)}, \quad l = 1, 2, \ldots, S. \quad (62)$$

Then, the BER at the kth subcarrier of the lth stratum becomes [22]

$$\mathrm{BER}_{l,k} = \frac{4}{\log_2 M_l}\left(1 - \frac{1}{\sqrt{M_l}}\right)\sum_{i=1}^{\sqrt{M_l}/2} Q\left((2i-1)\sqrt{\frac{3\left(2^{2l-1}\right)\pi\left(P_{\mathrm{o}}^{\mathrm{avg}}\right)^2\left|H_k\right|^2}{\left(M_l - 1\right)\left(B_{\mathrm{sc}} N_0 N \alpha_l^{\mathrm{o}}\right)}}\right). \quad (63)$$

The total theoretical BER bound of the lth stratum is then calculated by using the same formula as (46):

$$\mathrm{BER}_l = \frac{1}{N_l^{\mathrm{info}}}\sum_{k=1}^{\left(N_l/2\right)-1} \mathrm{BER}_{l,k}, \quad l = 1, 2, 3, \ldots, S. \quad (64)$$

The overall theoretical BER bound of STACO-ODM can be calculated by using similar formula defined on (47).

5. Simulation Results

The performance of the developed stratified ACO-OFDM (STACO-OFDM) is analyzed and compared with the performance of ACO-OFDM, DCO-OFDM, and eU-OFDM schemes for nonflat dispersive diffused optical wireless channel. Zero-forcing equalizer is used in all cases. The performance comparison is based on energy efficiency and BER performance over channels having different amount of delay spread and normalized channel impulse response (CIR). The simulation models used for comparisons (ACO/DCO-OFDM) are verified by simulation results presented in [12, 23] for the same parameters. The major simulation parameters are listed out in Table 1.

In the proposed STACO-OFDM and eU-OFDM schemes, the length of the cyclic prefix is set to be 32 for each subframes which are transmitted into two consecutive sessions. To achieve similar spectral efficiency for the three schemes and for fair comparison, 64 samples long cyclic prefix is used for ACO-OFDM and DCO-OFDM.

5.1. Channel Impulse Response (CIR). Figure 5 shows the discrete time simulation result of normalized time domain CIR of the diffused optical channel h_{n} for channel delay spread of 10 ns and 20 ns. The time duration between two discrete points is used to generate the channel samples with consideration of no blocking object which blocks the reflected light from arriving at the receiver. The result in Figure 5 confirms that 32 samples long cyclic prefix is enough to avoid ISI since the magnitude of h_{n} is almost zero for samples beyond the 12th sample. Figure 6 shows the plot of

Table 1: Major simulation parameters.

OFDM parameters			
IFFT/FFT size	2048		
Cyclic prefix length	64		
Sampling frequency (f_s)	100 MHz		
Channel delay spread (D_{rms})	10 ns, 20 ns		
Modulation techniques			
	Stratum-1	Stratum-2	Stratum-3
STACO-OFDM/ eU-OFDM	16-QAM 32-QAM 64-QAM	8-QAM 16-QAM 64-QAM	4-QAM 16-QAM 16-QAM
ACO-OFDM	64, 256, 1024-QAM		
DCO-OFDM	8, 16, 32-QAM		
Spectral efficiency	≈1.5, 2, and 2.5 bits/s/Hz		
Bit rate	145 Mbs, 194 Mbs, 242 Mbs		

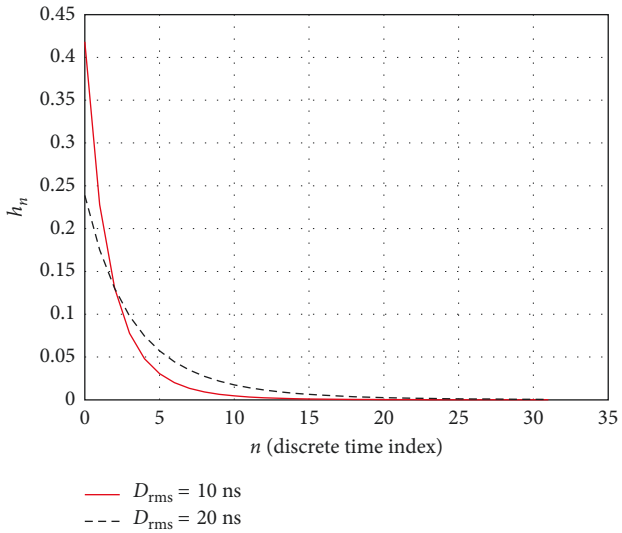

Figure 5: The normalized time domain CIR from ceiling bounce model for D_{rms} = 10, 20 ns.

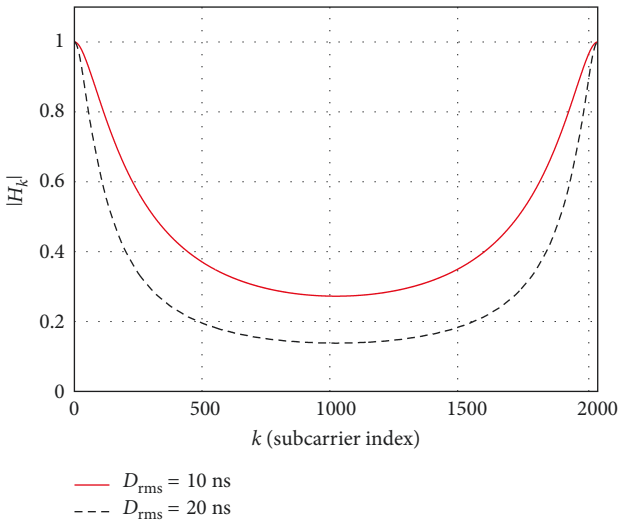

Figure 6: Frequency domain subcarrier gain for CIR with D_{rms} = 10, 20 ns.

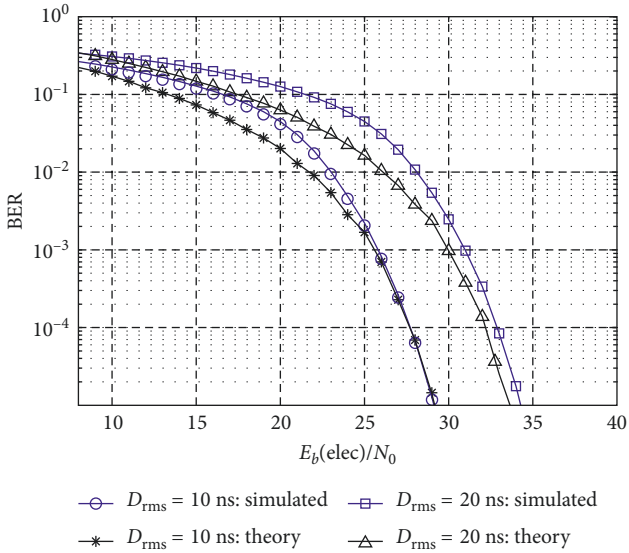

Figure 7: Theoretical and simulated BER of STACO-OFDM for spectral efficiency of 2 bits/s/Hz.

frequency domain subcarrier gain of the optical wireless channel for the normalized CIR with D_{rms} of (10 ns, 20 ns). As presented in Figure 5, the optical wireless channel has low pass nature and is becoming more frequency selective when the quantity of D_{rms} is increased. The subcarriers near to the zero frequency are relatively in better condition to achieve relatively better SNR since they have relatively higher channel gain. Moreover, while the channel delay spread is increasing, the channel gains of the subcarriers are decreasing; hence, it is difficult to achieve enough SNR for better BER performance while the quantity of the channel delay becomes large.

5.2. BER versus Electrical SNR per Bit. To compare the electrical energy efficiencies of the four schemes, the BER performances versus electrical E_b/N_0 are analyzed for all modulation schemes having similar spectral efficiencies and bit rates. As shown in Figure 7, the simulation result and the theoretical BER bound have shown good agreement apart from the inclusion of the residual error introduced by the successive demodulation on the simulated BER. The result in Figure 8 presented the comparison of the four schemes in terms of electrical energy efficiency for the system providing 1.5 bits/s/Hz and bit rate of 145 Mb/s over diffused optical channel. As the simulation result shows, to achieve a BER of 10^{-5} over multipath channel having delay spread of 10 and 20 ns, respectively, the proposed STACO-OFDM delivers electrical energy savings of about 1.7 and 1.6 dB compared to ACO-OFDM, about 4.8 and 5.5 dB electrical energy savings compared to DCO-OFDM, and about 1.2 and 1.6 dB electrical energy savings compared to eU-OFDM.

In Figure 9, the BER performance with respect to electrical SNR is presented for the four schemes providing spectral efficiency of 2 bits/s/Hz and a bit rate of 194 Mb/s. As the simulation result confirms, the performance of proposed STACO-OFDM scheme outsmarts the performances of ACO-OFDM, DCO-OFDM, and eU-OFDM for

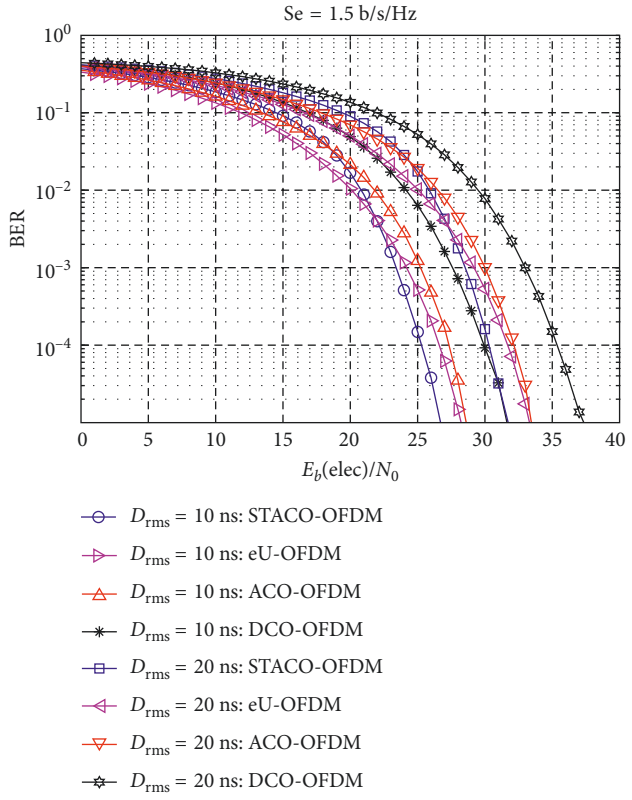

Figure 8: BER versus electrical SNR performance of STACO-OFDM, ACO-OFDM, and DCO-OFDM with spectral efficiency of 1.5 bits/s/Hz over multipath channel with D_{rms} = 10, 20 ns.

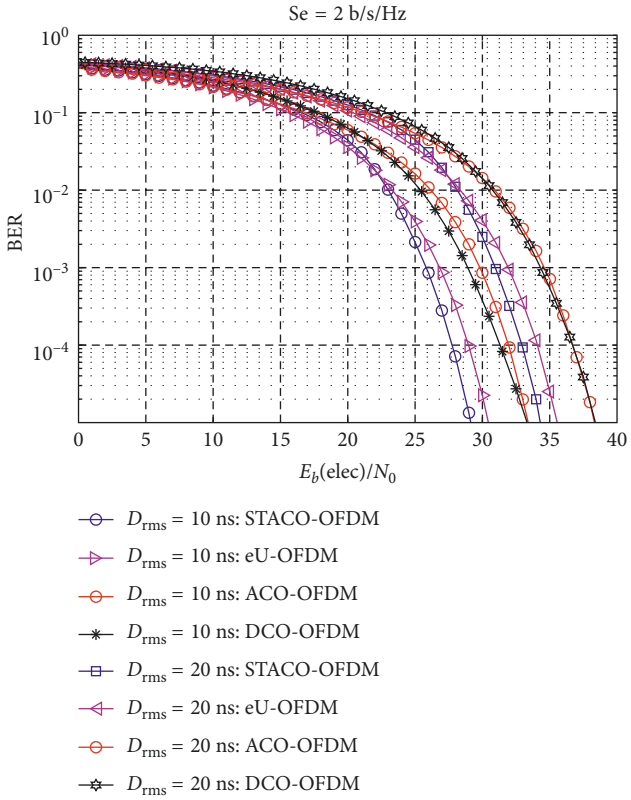

Figure 9: BER versus electrical SNR performance of STACO-OFDM, ACO-OFDM, and DCO-OFDM with spectral efficiency of 2 bits/s/Hz over multipath channel with D_{rms} = 10, 20 ns.

nonflat multipath channel with the given channel delay spreads. To achieve a BER of 10^{-5} over multipath channel having D_{rms} of 10 ns, STACO-OFDM provides electrical energy savings of about 4.3, 1.3, and 4.3 dB, respectively, compared to ACO-OFDM, eU-OFDM, and DCO-OFDM. To achieve the same BER (10^{-5}) on channel with D_{rms} of 20 ns, STACO-OFDM offers 4.1, 1.6, and 4.1 dB electrical energy savings compared to ACO-OFDM, eU-OFDM, and DCO-OFDM, respectively. The BER performances of the four schemes over multipath channel for system having spectral efficiency of 2.5 bits/s/Hz and bit rate of 242 Mb/s are presented in Figure 10. For the channel with D_{rms} of 10 ns, STACO-OFDM achieves BER of 10^{-5} with 6.1, 5, and 3.1 dB lower electrical energy consumption compared to ACO-OFDM, DCO-OFDM, and eU-OFDM, respectively. Similarly, for the second channel scenario (D_{rms} = 20 ns), the energy consumption of STACO-OFDM is lower by 5.9, 5.7, and 3.7 dB compared to ACO-OFDM, DCO-OFDM, and eU-OFDM, respectively.

The overall presented simulation results also show that when the spectral efficiency increases the SNR penalty of ACO-OFDM in comparison to STACO-OFDM is increased since higher order QAM modulations are used in ACO-OFDM to fill the spectral efficiency gap.

It is noted that higher order QAM modulation are not energy efficient. To achieve a better BER over multipath channel having relatively larger channel delay spread, the electrical power of the transmitted signal should be high to achieve enough SNR. But while increasing the electrical power of the transmitted signal, the peak of the negative samples also increase in the negative region, and this will introduce large clipping noise for the case of DCO-OFDM since most peaks are left in the negative region even after adding a DC bias. Thus, the presented simulation results show that DCO-OFDM is more affected by multipath fading due to the presence of unavoidable clipping noise. The presented results also revealed that the residual noise propagating from stratum to stratum during successive demodulation affects the energy efficiencies of STACO-OFDM and eU-OFDM for large channel delay spreads.

According to the results given on previous literatures [10, 16], both STACO-OFDM and eU-OFDM schemes have shown equivalent BER performances as a function of electrical SNR for a linear AWGN channel. Nevertheless, the results presented on this paper have shown that STACO-OFDM can offer somehow better BER performance compared to eU-OFDM on frequency selective multipath channel. As given in Figure 6, the optical wireless channel has low pass nature and the subcarriers on the high frequency region are more attenuated by the effect of the channel. eU-OFDM utilizes those subcarriers in the low and high frequency region at each layer for transmission of information bits. On the other hand, STACO-OFDM avoids utilizing those high frequency subcarriers on higher depth strata. Therefore, the usages of high frequency

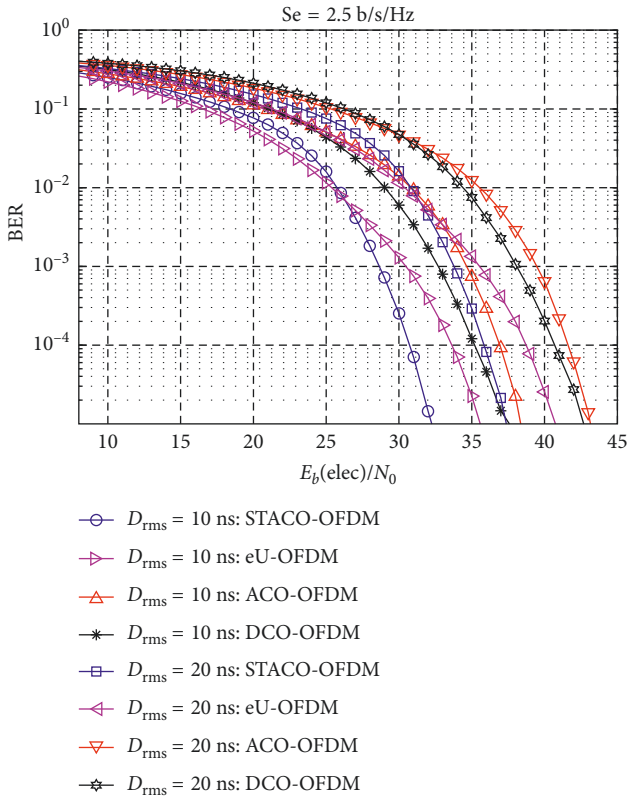

Figure 10: BER versus electrical SNR performance of STACO-OFDM, ACO-OFDM, and DCO-OFDM with spectral efficiency of 2.5 bits/s/Hz over multipath channel with D_{rms} = 10, 20 ns.

Table 2: Simulation parameters for BER versus optical power.

Simulation parameters	
DC channel gain (H_0)	10^{-6}
Noise spectral density (N_0)	3.05×10^{-23}
Transmitted optical power (P_o)	25–40 dBm

region subcarriers on all layers reduce the BER performance of eU-OFDM.

5.3. BER versus Optical Power. To evaluate the BER performance of STACO-OFDM scheme in terms of transmitted optical power, the parameters listed in Table 2 are used in addition to the main parameters listed in Table 1.

The channel parameters (D_{rms}, H_0, and N_0) in Table 2 for simulation are consistent with channel parameters presented on literature [1]. The results from numerical simulation and the theoretical BER bound given at (64) and (47) have shown good agreement as shown in Figure 11.

The BER versus P_o (transmitted optical power) performances of the three optical OFDM schemes over multipath channel having a delay spread of 10 ns are presented in Figures 12–14 for spectral efficiencies of 1.5, 2, and 2.5 bits/s/Hz, respectively. For a system delivering spectral efficiency of 1.5 bits/s/Hz, STACO-OFDM shows better performance with around 0.6 dB and 2.6 dB optical energy savings to achieve a BER of 10^{-5} compared to ACO-OFDM

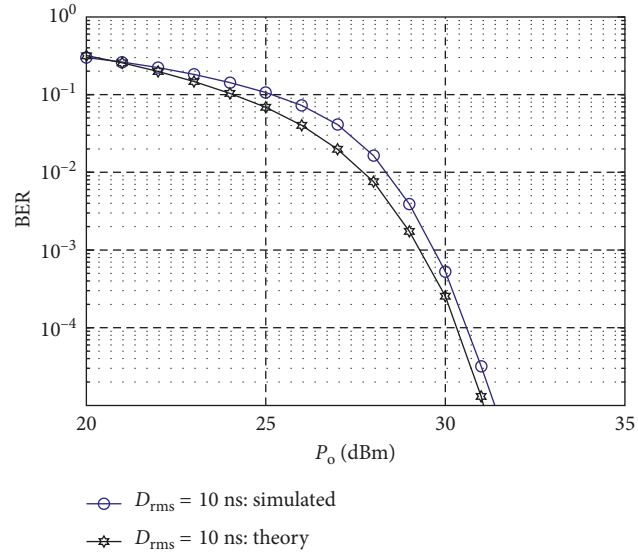

Figure 11: Theoretical and simulated BER of STACO-OFDM in terms of transmitted optical power for a system with spectral efficiency of 1.5 bits/s/Hz over multipath channel with D_{rms} of 10 ns.

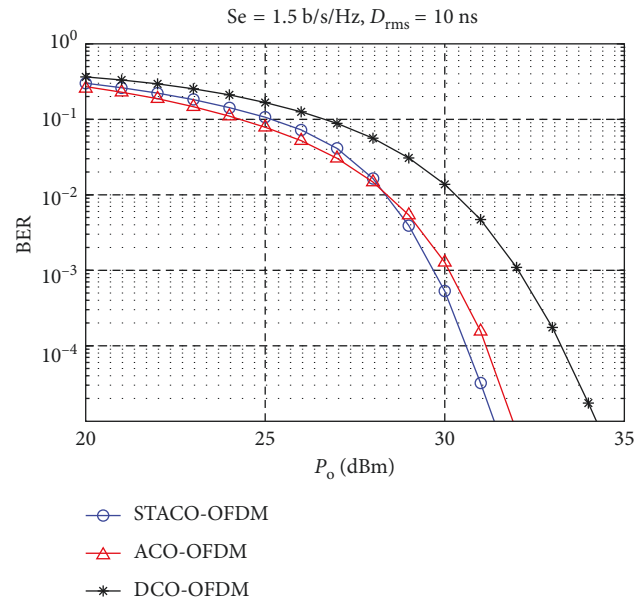

Figure 12: BER versus optical power performance of STACO-OFDM, ACO-OFDM, and DCO-OFDM with spectral efficiency of 1.5 bits/s/Hz over multipath channel with D_{rms} = 10 ns.

and DCO-OFDM, respectively, as shown in Figure 12. The simulation results in Figure 13 revealed that STACO-OFDM saves about 1.5 dB optical energy compared to ACO-OFDM and 2.5 dB optical energy compared to DCO-OFDM for the system offering spectral efficiency of 2 bits/s/Hz with a BER of 10^{-5}. The optical power penalty of ACO-OFDM with respect to STACO-OFDM is increased because of higher level QAM (256-QAM) usage to equalize the spectral efficiency of ACO-OFDM to 2 bits/s/Hz. Due to the energy inefficient properties of higher level QAM modulations, the

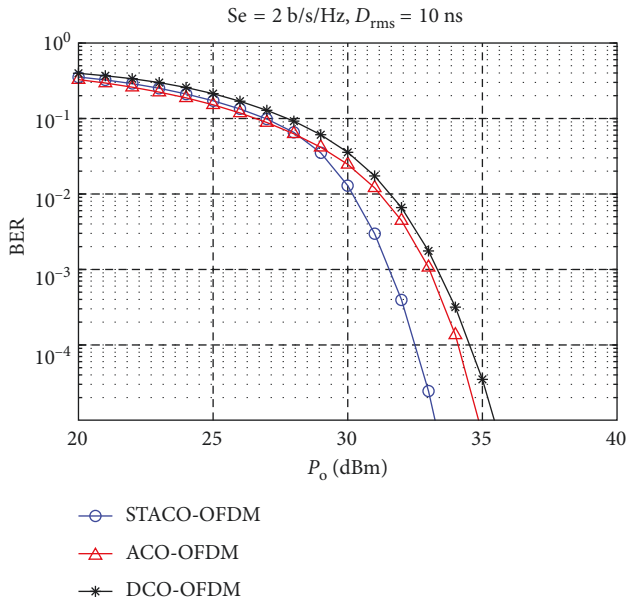

Figure 13: BER versus optical power performance of STACO-OFDM, ACO-OFDM, and DCO-OFDM with spectral efficiency of 2 bits/s/Hz over multipath channel with D_{rms} = 10 ns.

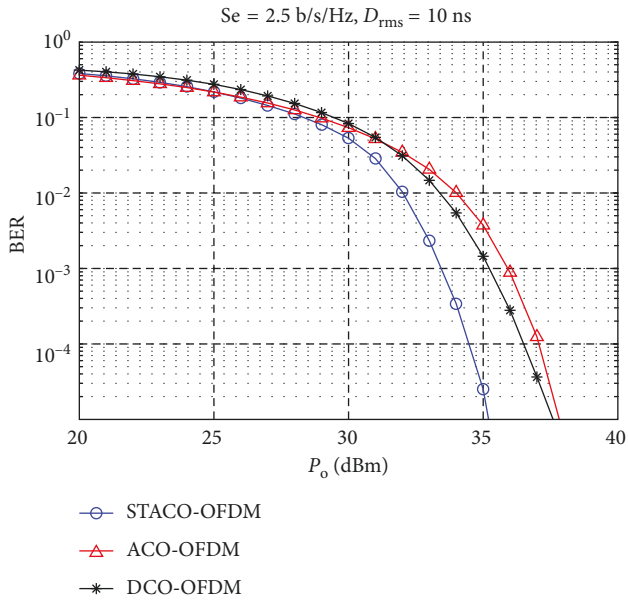

Figure 14: BER versus optical power performance of STACO-OFDM, ACO-OFDM, and DCO-OFDM with spectral efficiency of 2.5 bits/s/Hz over multipath channel with D_{rms} = 10 ns.

power penalty of ACO-OFDM has become large. Similarly, as the results in Figure 14 confirmed, the performance of STACO-OFDM outsmarts the performance of both ACO-OFDM and DCO-OFDM for the system providing a spectral efficiency of 2.5 bits/s/Hz.

To achieve a BER of 10^{-5}, STACO-OFDM requires 35.3 dBm optical power while DCO-OFDM and ACO-OFDM schemes require optical power of 37.6 dBm and 37.8 dBm, respectively. Therefore, compared to ACO/DCO-OFDM schemes, the overall presented results have shown that STACO-OFDM provides better optical power efficiency which has huge significance for solving drawbacks of optical power constraints to meet eye and skin safety regulations in indoor optical wireless communications.

6. Conclusions

The BER performance of the proposed STACO-OFDM is evaluated under the influence of multipath fading. Performance comparisons based on BER have been also made with ACO-OFDM, DCO-OFDM, and eU-OFDM. For systems providing similar bit rates, the results from simulation have confirmed that STACO-OFDM provides better energy efficiency and BER performances compared to ACO-OFDM, DCO-OFDM, and eU-OFDM over multipath channel. Moreover, STACO-OFDM has reduced communication latency compared to eU-OFDM scheme. The future research will focus on improving the performance of STACO-OFDM on frequency selective optical wireless channel by incorporating bit and power loading adaptive capabilities.

Conflicts of Interest

The authors declare that they have no conflicts of interest.

References

[1] J. M. Kahn and J. R. Barry, "Wireless infrared communications," *Proceedings of the IEEE*, vol. 85, no. 2, pp. 265–298, 1997.

[2] Y. Tanaka, T. Komine, S. Haruyama, and M. Nakagawa, "Indoor visible communication utilizing plural white LEDs as lighting," in *Proceedings of the 12th IEEE International Symposium on Personal, Indoor and Mobile Radio Communications (PIMRC 2001)*, vol. 2, pp. F-81–F-85, San Diego, CA, USA, September 2001.

[3] R. V. Nee and R. Prasad, *OFDM for Wireless Multimedia Communications*, Artech House, Norwood, MA, USA, 2000.

[4] T. Ohtsuki, "Multiple-subcarrier modulation in optical wireless communications," *IEEE Communications Magazine*, vol. 41, pp. 74–79, 2003.

[5] O. Gonzalez, R. Perez-Jimenez, S. Rodriguez, J. Rabadan, and A. Ayala, "OFDM over indoor wireless optical channel," *IEE Proceedings–Optoelectronics*, vol. 152, no. 4, pp. 199–204, 2005.

[6] J. Armstrong and B. Schmidt, "Comparison of asymmetrically clipped optical OFDM and DC-biased optical OFDM in AWGN," *IEEE Communications Letters*, vol. 12, no. 5, pp. 343–345, 2008.

[7] J. Armstrong, "OFDM for optical communications," *Journal of Light Wave Technology*, vol. 27, no. 3, pp. 189–204, 2009.

[8] J. Armstrong and A. Lowery, "Power efficient optical OFDM," *Electronics Letters*, vol. 42, no. 6, pp. 370–372, 2006.

[9] N. Fernando, H. Yi, and E. Viterbo, "Flip-OFDM for unipolar communication systems," *IEEE Transactions on Communications*, vol. 60, no. 12, pp. 3726–3733, 2012.

[10] Z. Hailu, K. Langat, and C. Maina, "Stratified ACO-OFDM modulation for simultaneous transmission of multiple frames both on even and odd subcarriers," *Journal of Communications*, vol. 12, no. 5, pp. 261–270, 2017.

[11] D. Tsonev, S. Videv, and H. Haas, "Unlocking spectral efficiency in intensity modulation and direct detection systems,"

IEEE Journal on Selected Areas in Communications, vol. 33, no. 9, pp. 1758–1770, 2015.

[12] J. Panta, P. Saengudomlert, and K. Sripimanwat, "Performance improvement of ACO-OFDM indoor optical wireless transmissions using partial pre-equalization," *ECTI Transactions on Electrical Engineering, Electronics, and Communications*, vol. 14, no. 1, pp. 1–11, 2015.

[13] S. K. Wilson and J. Armstrong, "Transmitter and receiver methods for improving asymmetrically clipped optical OFDM," *IEEE Transactions on Wireless Communications*, vol. 8, no. 9, pp. 4561–4567, 2009.

[14] S. Dimitrov, H. Haas, M. Cappitelli, and M. Olbert, "On the throughput of an OFDM-based cellular optical wireless system for an aircraft cabin," in *Proceedings of the 5th European Conference on Antennas and Propagation (EuCAP 2011)*, Rome, Italy, April 2011.

[15] X. Li, J. Vucic, V. Jungnickel, and J. Armstrong, "On the capacity of intensity-modulated direct-detection systems and the information rate of ACO-OFDM for indoor optical wireless applications," *IEEE Transactions on Communications*, vol. 60, no. 3, pp. 799–809, 2012.

[16] M. Islim, D. Tsonev, and H. Haas, "A generalized solution to the spectral efficiency loss in unipolar optical OFDM-based systems," in *Proceedings of the IEEE International Conference on Communications*, pp. 5126–5131, London, UK, 2015.

[17] L. Rugini, P. Banelli, and G. Leus, "OFDM Communications over time-varying channels," in *Wireless Communications over Rapidly Time-Varying Channels*, pp. 285–297, Academic Press, Oxford, UK, 1st edition, 2011.

[18] B. Muquet, Z. Wang, G. B. Giannakis, M. de Courville, and P. Duhamel, "Cyclic prefixing or zero padding for wireless multicarrier transmissions?," *IEEE Transactions on Communications*, vol. 50, no. 12, pp. 2136–2148, 2002.

[19] P. Saengudomlert, "On the benefits of pre-equalization for ACO-OFDM and flip-OFDM indoor wireless optical transmissions over dispersive channels," *Journal of Lightwave Technology*, vol. 32, no. 1, pp. 70–80, 2014.

[20] X. Li, R. Mardling, and J. Armstrong, "Channel capacity of IM/DD optical communication systems and of ACO-OFDM," in *Proceedings of the IEEE International Conference on Communications*, Glasgow, UK, June 2007.

[21] J. Burkardt, *The Truncated Normal Distribution*, in press.

[22] F. Xiong, *Digital Modulation Techniques*, chapter 9, Artech House, Norwood, MA, USA, 2nd edition, 2006.

[23] T. Kozu and K. Ohuchi, "BER performance of Superposed ACO-OFDM in multi-path fading channel," in *Proceedings of the IEEE International Symposium on Signal Processing and Information Technology (ISSPIT)*, Limassol, Cyprus, December 2016.